the internal environment of HCC patients with chronic hepatitis C (CH-C) infection.

Materials and Methods

Study subjects. All patients participating in this study had advanced chronic liver disease, cirrhosis, or persistent HCV infection. Twelve patients who developed HCC as a consequence of advanced chronic liver disease related to hepatitis C and who underwent surgical treatment were enrolled (Supplementary Table S1). HCC and noncancerous liver tissues were obtained and frozen. For analysis of gene expression profiles in PBMCs, 32 LC patients without HCC and 30 LC patients with HCC (Supplementary Table S2) were included. Development of HCC was diagnosed by computed tomography (CT) or magnetic resonance imaging with contrast reagents and abdominal angiography with CT imaging in arterial and portal flow phases (18). The pathologic tumor node metastasis classification system of the Liver Cancer Study Group of Japan was used for the staging of HCC. LC was diagnosed by pathologic findings in biopsy specimens where available; otherwise, radiological imaging, platelet counts, serum hyaluronic acid levels, and indocyanine green retention rates were considered for the diagnosis of cirrhosis. The study has been approved by the institutional review board, and informed consent was obtained from all patients enrolled in the study.

Isolation of PBMCs. PBMCs were isolated from heparinized blood samples by Ficoll-Hipaque density gradient centrifugation, as reported previously (15).

Laser capture microdissection. HCC and noncancerous liver tissues obtained during surgery were frozen in optimum cutting temperature compound (Sakura Finetech; ref. 13). All HCC tissues were nodular and clearly separated by noncancerous tissues macroscopically. Cells infiltrating HCC tissues were visualized under a microscope and precisely excised by laser capture microdissection (LCM) using a CRI-337 (Cell Robotics, Inc.), as previously performed (Supplementary Fig. S1*A*; ref. 12). Cells infiltrating noncancerous tissues of CH-C patients were visualized and excised similarly.

RNA isolation and amplification. Total RNA was isolated from PBMCs or tissue samples using a microRNA isolation kit (Stratagene) in accordance with the supplied protocol with slight modifications. Isolated RNA was then amplified twice using antisense RNA and an Amino Allyl MessageAmp aRNA kit (Ambion), as described previously (13). The reference RNA sample was isolated from the PBMCs of a 29-yr-old healthy male volunteer and was amplified in the same manner. Amplified RNAs from the PBMCs of patients and the healthy volunteer were labeled with Cy5 and Cy3 (Amersham), respectively. Equal amounts of amplified RNAs were hybridized to an oligo-DNA chip (AceGene Human Oligo Chip 30K, Hitachi Software Engineering Co., Ltd.) overnight and were then washed for image scanning.

DNA microarray image analysis. The fluorescence intensity of each spot on the oligo-DNA chip was determined using a DNA Microarray Scan Array G (PerkinElmer). The images obtained were quantified using a DNASIS array (v2.6, Hitachi Software Engineering Co., Ltd). For normalization, the intensity of each spot without oligo-DNA was subtracted from that with oligo-DNA in the same block. A validated spot was determined when the intensity of the spot was within the intensity ± 2 SDs for each block. By calibrating the median to base quantity, the intensities of all spots were adjusted for normalization between Cy5 and Cy3.

Quantitative real-time detection PCR. Real-time detection PCR (RTD-PCR) was performed as previously described (15). Briefly, template cDNA was synthesized from 1 μg of total RNA using SuperScript II RT (Invitrogen). Primer pairs for chemokine (C-C motif) receptor 1 (*Ccr1*), histone acetyltransferase 1 (*Hat1*), mitogen-activated protein kinase kinase 1 interacting protein 1 (*Map2k1ip1*), phosphatidylinositol glycan anchor biosynthesis, class B (*PigB*), toll-like receptor 2 (*Tlr2*), superoxide dismutase 2 (*Sod2*), cytokeratin 8 (*Krt8*), *Krt18*, *Krt19*, and glyceraldehydes-3-phosphate dehydrogenase, as an internal control of expression, were purchased from the TaqMan assay reagents library (Applied Biosystems). Synthesized cDNA was mixed with the TaqMan Universal Master Mix (Applied Biosystems), as well as each primer pair and reaction was performed using ABI PRISM 7900HT. Relative expression level of each gene was calculated compared with that of internal control in each sample. Results are expressed as means ± SE.

Flow cytometry analysis. Flow cytometry analysis was performed as described previously (19). Briefly, isolated PBMCs were incubated in PBS supplemented with 2% bovine serum albumin (Sigma-Aldrich JAPAN K.K.) with antihuman CCR1 and CCR2 antibodies labeled with Alexa Fluor 647 (Becton Dickinson Pharmingen). The fluorescence intensity of the cells was measured using a FACSort (Becton Dickinson).

Immunohistochemistry. Surgically obtained HCC and noncancerous liver tissues were fixed with neutral buffered formalin, embedded in paraffin, cut into 4-μm sections, and mounted on microscope slides. The fixed slides were deparaffinized and subjected to heat-induced epitope retrieval 98°C for 40 min. After blocking endogenous peroxidase activity in the tissue specimen using 3% hydrogen peroxide, the slides were incubated with appropriately diluted primary antibodies, antihuman CD4 or anti-human CD14 mouse monoclonal antibodies (Visionbiosystems Novocastra). The reaction was visualized by the REAL EnVision Detection System (DAKO) followed by counterstaining with hematoxylin.

Statistical analysis. Hierarchical clustering and principal component analysis of gene expression was performed using BRB-ArrayTools.[1] Fisher's exact test was used to examine the significance of hierarchical clustering in the dendrogram. A class prediction was performed by three nearest neighbors, incorporating genes that were differentially expressed at the $P = 0.002$ significance level, as assessed by the random variance t test (BRB-ArrayTools). For genes to analyze in a pathway, we used a P value of <0.05 with 2,000 permutations to avoid underestimating the presence of meaningful signaling pathways that were coordinately up-regulated or down-regulated with subtle differences (13). The cross-validated misclassification rate was computed, and at least 2,000 permutations were performed for a valid permutation P value. The univariate t values for comparing the classes were used as weights. Student's t-test was performed for RTD-PCR data, and P values of <0.05 were deemed to be statistically significant. The population of CCR1-positive or CCR2-positive cells in PBMCs by flow cytometry analysis was tested for differences (with $P < 0.05$) by the Mann-Whitney U-test, using SPSS software (SPSS Japan, Inc.).

Analysis of expression data for biological processes and networks. As for genes significantly up-regulated or down-regulated in HCC-infiltrating mononuclear inflammatory cells compared with noncancerous liver-infiltrating mononuclear inflammatory cells or in PBMCs in LC without HCC compared with LC with HCC at $P < 0.05$, we have performed analysis of the biological processes using the MetaCore software suite (GeneGo), as described previously (13). Possible networks were created according to the list of the differentially expressed genes using the MetaCore database, a unique curated database of human protein-protein and protein-DNA interactions, transcription factors, and signaling, metabolic, and bioactive molecules. The P value was calculated as described previously (13).

Gene expression data of major leukocyte types and analysis of DNA microarray expression data. Gene expression data for leukocytes were retrieved through publicly accessible databases.[2] The gene set database GDS1775, which includes gene expression data for major leukocyte types, was obtained and subjected to one-way clustering analysis using BRB-Array Tools with genes that were up-regulated in HCC-infiltrating mononuclear inflammatory cells for the enrolled cases above.

Results

Gene expression in mononuclear inflammatory cells infiltrating into HCC tissue. HCC is frequently associated with infiltrating mononuclear inflammatory cells (20), and various attempts have been made to understand their biological significance

[1] http://linus.nci.nih.gov/BRB-ArrayTools.html
[2] http://www.ncbi.nlm.nih.gov/geo/

(8, 9, 21). We selectively obtained HCC-infiltrating mononuclear inflammatory cells by LCM and compared their gene expression profiles with those of noncancerous liver-infiltrating mononuclear inflammatory cells obtained in the same way (Supplementary Fig. S1*A*; Supplementary Table S1). The gene expression profiles of HCC-infiltrating mononuclear inflammatory cells showed that 115, 206, and 773 genes were up-regulated and 52, 114, and 750 genes were down-regulated compared with those of noncancerous liver-infiltrating mononuclear inflammatory cells at P levels of <0.005, <0.01, and <0.05, respectively (Geo accession no.[3] GSE 10461; Supplementary Fig. S1*B*).

Genes at the $P < 0.05$ level were analyzed with regard to their role in biological processes in HCC-infiltrating mononuclear inflammatory cells compared with noncancerous liver-infiltrating mononuclear inflammatory cells using the MetaCore pathway analysis software. The significant processes, in which the up-regulated genes in HCC-infiltrating mononuclear inflammatory cells were involved, included antigen presentation, an immunologically important process in antigen-presenting cells, such as monocyte/macrophages and dendritic cells (Table 1; ref. 22). The genes involved in this process were the genes for the CD1d molecule and C-type lectin domain family 4 for glycolipid antigen recognition (23, 24) and CD86, an accessory molecule indispensable for provoking an immune response (25), suggesting an activated immune reaction in these cells. The up-regulated genes in HCC-infiltrating mononuclear inflammatory cells were also involved in the ubiquitin-proteasomal proteolysis process, with significant genes, such as those encoding ubiquitin-conjugating enzymes and proteasome subunits. This process is required to eradicate unnecessary proteins, which are ubiquitinated, and then degraded in proteasomes (26). Processes related to the steps of gene expression, such as transcription by RNA polymerase II, mRNA processing, and the process of the cell cycle were also represented in the genes up-regulated in HCC-infiltrating mononuclear inflammatory cells, indicating enhanced cellular activity. Genes involved in the process of double-strand breaks, such as topoisomerase II α4 (27), and proliferating cell nuclear antigen (PCNA; ref. 28) genes involved in responses to hypoxia and oxidative stress, such as thioredoxin, peroxiredoxin, and antioxidant protein, were also up-regulated, suggesting that HCC-infiltrating mononuclear inflammatory cells were in an activated inflammatory status and under hypoxic or oxidative stress, presumably caused by the HCC. Thus, the profile of up-regulated genes in HCC-infiltrating mononuclear inflammatory cells suggested an inflammatory status, possibly triggered by antigenic stimulation of HCC tissues.

Fewer processes were identified for the down-regulated genes. One intriguing process identified was that of integrin-mediated cell matrix adhesion, suggesting that HCC-infiltrating mononuclear inflammatory cells may be less adhesive in the local tissues where they were found (Supplementary Table S3).

Subpopulation analysis of HCC-infiltrating mononuclear inflammatory cells using immunohistochemistry and transcriptional analysis. Tumor-infiltrating mononuclear inflammatory cells consist of a mixed cell population, including macrophages, effector T cells, and regulatory T cells, which have been considered to be both cancer-favorable or cancer-unfavorable (8, 21). HCC-infiltrating and noncancerous liver-infiltrating mononuclear inflammatory cells were immunohistochemically evaluated to examine the characteristics of the subpopulations. CD14-positive monocytes/macrophages were prominent in HCC-infiltrating mononuclear inflammatory cells, whereas they were rarely observed in noncancerous liver-infiltrating mononuclear inflammatory cells (Fig. 1*A*). CD4-positive helper T cells were observed in both HCC tissues and noncancerous liver tissues, although in noncancerous liver tissues, these cells tended to accumulate within the aggregates of mononuclear inflammatory cells, whereas they seemed to be scattered in HCC-infiltrating mononuclear inflammatory cells (Fig. 1*A*).

Next, we examined the genes that were significantly up-regulated in HCC-infiltrating mononuclear inflammatory cells compared with noncancerous liver-infiltrating mononuclear inflammatory cells, relative to subpopulations of leukocytes, and explored how they may be relevant to leukocyte subpopulations, using the database of the human immune cell transcriptome in the Gene Expression Omnibus[3] (Geo accession no. GDS1775), which covers 26 immune regulatory cells, such as T cells, B cells, natural killer cells, macrophages, dendritic cells, basophils, and eosinophils. Among the 206 extracted, up-regulated genes in HCC-infiltrating mononuclear inflammatory cells (at the $P < 0.01$ level), 97 annotated genes were used for one-way hierarchical clusters (Fig. 1*B*). Most genes among 97 annotated up-regulated genes in HCC-infiltrating mononuclear inflammatory cells were shown to be expressed with higher magnitude in lipopolysaccharide-stimulated or lipopolysaccharide-unstimulated macrophages than in other types of major leukocytes. The next subpopulations, including the second most number of genes for relatively high magnitude of expression, were Th1 and Th2 CD4 cells under conditions supplemented with interleukin-12 (IL-12) and IL-4, respectively (Geo accession no.[3] GSM90858), secreting Th1 and Th2 cytokine profiles, respectively, suggesting that featured genes expressed in HCC-infiltrating mononuclear inflammatory cells were indicative of CD4 helper T cells, secreting a variety of cytokines.

Thus, this expression analysis showed that, in HCC lesions with tumor antigens, there was an accumulation of antigen-presenting cells, monocyte/macrophages, and CD4 helper T cells, which were in a cytokine-secreting condition, with enhanced cellular biological activities, including ubiquitin-proteasomal proteolysis, presumably under a hypoxic and oxidative stress environment caused by the HCC. The overall inflammatory status represented by HCC-infiltrating mononuclear inflammatory cells was not determined in terms of an anticancer effect, because no obvious shift of CD4 helper T cells to the Th1 or Th2 condition was indicated.

Distinct gene expression profile of PBMCs obtained from patients with cirrhotic liver disease complicated with HCC. The HCC-infiltrating mononuclear inflammatory cells were distinct in terms of expressed genes. The putative biological processes involving these up-regulated genes in tumor-infiltrating mononuclear inflammatory cells suggested a general influence of the HCC on the local environment of the host, represented by stress-response genes. We, thus, examined whether PBMCs in the systemic circulation of the patient might also be influenced by the development of HCC. PBMCs were obtained from 30 patients with LC associated with HCC and from 32 patients with LC not associated with HCC, and the gene expression profiles were compared (Geo accession no.[3] GSE10459).

Unsupervised hierarchical clustering analysis using 17,903 filtered genes, the expression values of which were not missing in >50% of the cases, identified two major clusters of patients, with and without HCC (data not shown). To examine the reproducibility and the reliability of the clustering, we excluded

Table 1. Biological processes for genes up-regulated in HCC-infiltrating mononuclear inflammatory cells

Biological process	−log(*P*)	Gene	ID	*t* (*T/†NT)	*P*	Cellular components‡
Antigen presentation	8.526	CD163	NM_004244	3.96	0.001	M
		CD86 antigen	NM_006889	3.28	0.006	M
		IFN, α-inducible protein 6	NM_022872	2.99	0.031	M
		IFN, γ-inducible protein 30	NM_006332	2.89	0.011	M
		Fc fragment of IgG, high affinity Ia, receptor (CD64)	NM_000566	2.85	0.013	M
		C-type lectin domain family 4, member M	NM_014257	2.73	0.020	
		CD63	NM_001780	2.51	0.024	M
		CD1D antigen	NM_001766	2.19	0.049	
Ubiqutin-proteasomeal proteolysis	6.555	Nucleoporin 107 kDa	NM_020401	4.32	0.001	
		Proteasome subunit, β type, 5	NM_002797	3.80	0.002	T, M
		Ubiquitin-conjugating enzyme E2R 2	NM_017811	3.67	0.004	
		Proteasome subunit, α type, 5	NM_002790	3.64	0.003	
		Prostaglandin E synthase 3	NM_006601	3.53	0.003	
		Ubiquitin-conjugating enzyme E2 binding protein, 1	NM_005744	2.94	0.011	
		Ubiquitin-conjugating enzyme E2E 3	NM_006357	2.75	0.017	
		DnaJ (Hsp40) homologue, subfamily A, member 1	NM_001539	2.47	0.028	
		Syntaxin 5	BC012137	2.19	0.046	
ER and cytoplasm	5.704	Chaperonin containing TCP1, subunit 8 (θ)	NM_006585	3.71	0.002	T, M
		Peptidylprolyl isomerase A	NM_021130	3.69	0.002	
		ERO1-like	NM_014584	3.03	0.009	T, M
		Peptidylprolyl isomerase C	BC002678	2.68	0.017	M
		SEC63 homologue	AF119883	2.59	0.020	
		Peptidylprolyl isomerase B	NM_000942	2.54	0.023	
		Chaperonin containing TCP1, subunit 4 (δ)	NM_006430	2.53	0.023	
		FK506 binding protein 3, 25 kDa	NM_002013	2.46	0.026	T, M
		Heat shock 70 kDa protein 5	AF188611	2.45	0.027	
mRNA processing	5.143	Small nuclear ribonucleoprotein polypeptide B	NM_003092	4.65	0.000	
		Small nuclear ribonucleoprotein polypeptide F	BC002505	3.28	0.005	T
		DEAD (Asp-Glu-Ala-Asp) box polypeptide 20	NM_007204	3.22	0.006	
		Cleavage and polyadenylation specific factor 6	NM_007007	3.16	0.010	
		Cleavage stimulation factor subunit 2	NM_001325	3.10	0.008	T
		Heterogeneous nuclear ribonucleoprotein A2/B1	NM_031243	2.94	0.010	
		PRP4 pre-mRNA processing factor 4 homologue B	NM_003913	2.90	0.020	
		Gem-associated protein 4	NM_015721	2.64	0.019	T
		LSM6 homologue	NM_007080	2.63	0.019	
		Exportin 1	NM_003400	2.42	0.029	
		RNA-binding motif protein 8A	AF127761	2.41	0.030	
		Splicing factor, arginine/serine-rich 1	M72709	2.39	0.036	
Transcription by RNA polymerase II	4.298	TAF9 RNA polymerase II	NM_016283	5.01	0.001	
		General transcription factor IIH, polypeptide 3, 34 kDa	NM_001516	4.74	0.001	
		TAF6-like RNA polymerase II	NM_006473	3.91	0.002	
		Nuclear receptor corepressor 1	AF044209	3.64	0.007	
		TATA box binding protein	NM_003194	2.89	0.018	

(*Continued on the following page*)

Table 1. Biological processes for genes up-regulated in HCC-infiltrating mononuclear inflammatory cells (Cont'd)

Biological process	−log(*P*)	Gene	ID	*t* (*T/†NT)	*P*	Cellular components‡
		Cofactor required for Sp1 transcriptional activation	NM_004270	2.82	0.014	T, M
		SUB1 homologue	NM_006713	2.59	0.021	
		General transcription factor II, I	NM_033001	2.55	0.023	T, M
		GCN5-like 2	NM_021078	2.34	0.048	
		TBP-like 1	NM_004865	2.24	0.043	
Double-strand breaks repair	3.289	RAD51 homologue C	NM_058216	5.24	0.000	T
		Werner syndrome	AF091214	4.99	0.000	T
		NIMA-related kinase 1	AK027580	3.27	0.007	
		Protein phosphatase 2	AF086924	3.24	0.023	
		Protein phosphatase 6	NM_002721	3.13	0.007	
		Proliferating cell nuclear antigen	NM_002592	2.80	0.014	T
		Topoisomerase II α-4	AF285159	2.57	0.033	T
ESR1-nuclear pathway	2.886	Nuclear receptor corepressor 1	AF044209	3.64	0.007	
		Nuclear receptor coactivator 4	X77548	3.19	0.007	
		Dopachrome tautomerase	NM_001922	3.04	0.019	
		COP9, subunit 5	NM_006837	2.77	0.014	
		Tissue specific extinguisher 1	NM_002734	2.70	0.018	M
		SCAN domain containing 1	NM_033630	2.50	0.026	
		Kinase insert domain receptor	NM_002253	2.35	0.047	
Cell cycle	2.241	Cyclin-dependent kinase inhibitor 3	NM_005192	4.60	0.000	
		Erythrocyte membrane protein band 4.1	NM_004437	3.47	0.014	
		RAN, member RAS oncogene family	NM_006325	3.38	0.004	T
		Cyclin C	NM_005190	3.14	0.008	
		Cell division cycle 42	NM_044472	3.14	0.007	
		Cyclin-dependent kinase-like 1	NM_004196	2.77	0.033	
		Cell division cycle 73	NM_024529	2.72	0.043	M
		Cell division cycle 27	NM_001256	2.57	0.043	
		Microtubule-actin cross-linking factor 1	AK023285	2.57	0.025	
		Histone cluster 1	NM_005323	2.30	0.047	
		Cyclin-dependent kinase 7	NM_001799	2.13	0.050	
		Cyclin G_2	NM_004354	2.48	0.038	
Response to hypoxia and oxidative stress	1.401	Thioredoxin	NM_003329	2.64	0.019	T, M
		Glutaredoxin 2	NM_016066	2.63	0.024	T, M
		Peroxiredoxin 3	NM_006793	2.81	0.016	T, M
		Peroxiredoxin 2	NM_005809	2.27	0.039	
		Antioxidant protein 2	NM_004905	2.22	0.042	
		Peroxiredoxin 1	NM_002574	2.21	0.043	T, M
		Microsomal glutathione *S*-transferase 2	NM_002413	2.41	0.031	M

*T represents tumor-infiltrating mononuclear inflammatory cells.
†NT represents non-tumor-infiltrating mononuclear inflammatory cells.
‡Cellular components predominantly expressed cellular components among 26 immune regulatory cells (T, Th cells; M, macrophage).

unchanged genes in all samples (genes with less than a 1.8-fold difference in >85% of samples) to remove noise. This hierarchical clustering analysis using 1,917 filtered genes confirmed two clear clusters in patients with or without HCC (Fig. 2*A*). In one major cluster, including the most LC cases, there was a subcluster, LC/HCC, which included more of the HCC patients located next to the cluster of patients with HCC (LC/HCC; Fig. 2*A*). The reproducibility of the clustering (proportion, averaged over replications and over all pairs of samples in the same cluster, BRB-ArrayTools) was 93%. Sensitivity and specificity to HCC in this cluster analysis is 88% and 76%, respectively. These cirrhotic patients without HCC were followed for at least a further 12 months to detect HCC; none of those in the LC group developed HCC over this time. The principal component analysis was performed with the filtered 1,917 genes and the two major groups; classifying LC and HCC were similarly observed (Fig. 2*B*).

To further confirm that gene expression in the PBMCs of patients with HCC was distinct from that in patients without HCC, analysis of PBMC gene expression was performed by a

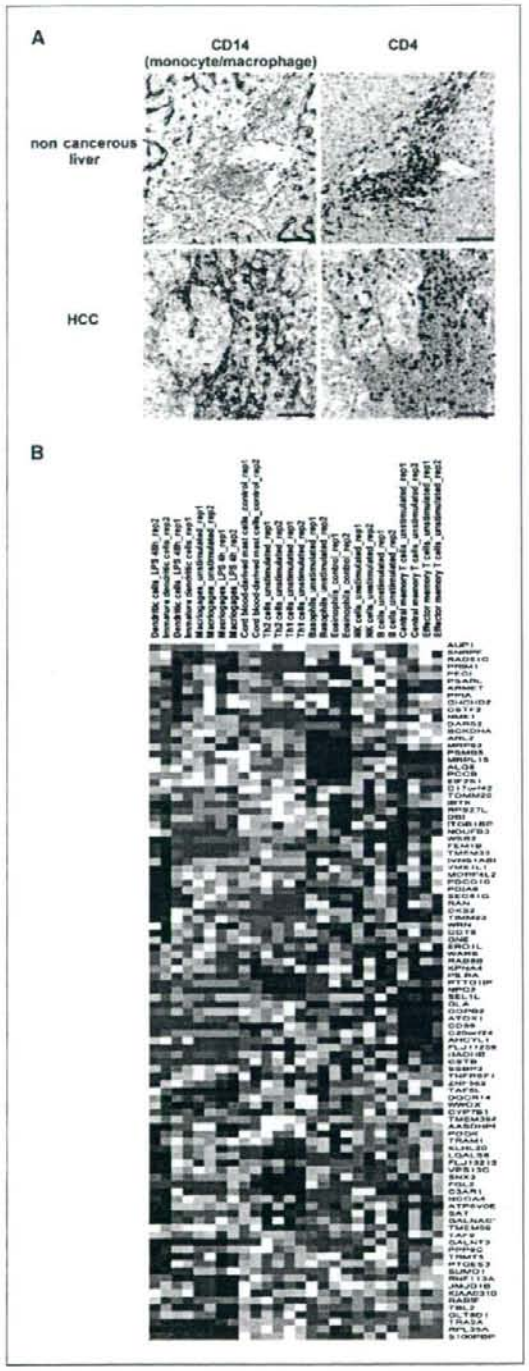

supervised learning method using categories of LC-C or HCC, age, gender, serum alanine aminotransferase (ALT), and α-fetoprotein (AFP). It showed that patients with or without HCC were significant classifiers ($P < 0.0005$), assigned with 1,430 predictor genes ($P < 0.002$; Table 2). Of 32 patients with LC, eight (25%) were misclassified as having HCC, and 2 of 30 patients with HCC (6.7%) were misclassified as not having HCC, indicating that the overall accuracy of the prediction of a patient with or without HCC was 84% (Table 2). Other clinical variables supposed to be related to HCC occurrence, such as age (ref. 29; >68 or ≤ 68 years old), gender (30), and ALT(ref. 31; >50 or ≤50 IU/L), could not differentiate gene expression in PBMCs. AFP (>20 or ≤20 ng/mL) was actually significant but was a much less powerful classifier ($P < 0.02$, assigned with 301 classifier genes). The prediction accuracy for categories of LC-C versus HCC and the AFP value >20 versus ≤20 ng/mL is not significantly affected whenever the number of predictor genes is reduced to below 62 (Supplementary Fig. S2). Taken together, these results by unsupervised and supervised analysis methods indicate that HCC development in LC-C patients significantly affects the gene expression profile in PBMCs.

Features of biological processes for which gene expression was significantly altered in PBMCs in HCC patients. We next examined the biological processes possibly affected by HCC development, given the expression profiles in PBMCs from patients with HCC. Statistical analysis showed that 867 genes were up-regulated and 989 genes were down-regulated in PBMCs from patients with HCC, compared with those without HCC ($P < 0.005$). Six representative genes, *Ccr1, Hat, Map2k1ip1, PigB, Tlr2,* and *Sod2,* were randomly selected from genes which were biologically important and differentially expressed between LC and HCC groups, and their expression was confirmed by RTD-PCR (Supplementary Fig. S3*A*). To exclude the possibility of circulating cancer cells, we have also examined the expression of *Afp, Krt8, Krt18,* and *Krt19*. No expression was detected for *Afp* (data not shown), and no statistically significant difference was found for expression of *Krt8, Krt18,* and *Krt19* between patients with HCC and without HCC (Supplementary Fig. S3*A*). The expression data were also confirmed by flow cytometric analysis. We evaluated how many cells in blood expressed CCR1 and CCR2 and confirmed that populations expressing CCR1 and CCR2 were significantly higher in PBMCs from patients with HCC than those without (Supplementary Fig. S3*B*). To understand the biological processes in PBMCs for which up-regulated or

Figure 1. HCC-infiltrating mononuclear inflammatory cells involve monocyte/macrophage and helper T cell. *A*, immunohistochemical staining. Many of the HCC-infiltrating mononuclear inflammatory cells expressed monocyte/macrophage marker, CD14. In contrast, few CD14-positive cells were seen in noncancerous liver-infiltrating mononuclear inflammatory cells. *Bars*, 100 μm. *B*, one-way hierarchical clustering analysis of gene expression of immune-mediating cells with genes whose expression was up-regulated in HCC-infiltrating mononuclear inflammatory cells. Data for gene expression in immune-mediating cells were retrieved from Gene Expression Omnibus[2] (Geo accession no. GDS 1775). By excluding genes missing from over half of the immune-mediating cells, 206 genes up-regulated in HCC-infiltrating mononuclear inflammatory cells were filtered, and the remaining 97 genes were used for clustering. Transverse and longitudinal titles show the type of immune-mediating cell and gene symbols, respectively. Color indicates relative expression magnitude of 97 up-regulated genes HCC-infiltrating mononuclear inflammatory cells among retrieved expression data of major leukocyte types deposited in the public database. The red and blue color means relatively high or low magnitude of expression among 26 retrieved expression data of leukocytes. The heat-map shows that helper T cells and unstimulated or stimulated macrophages included more blocks with the red color.

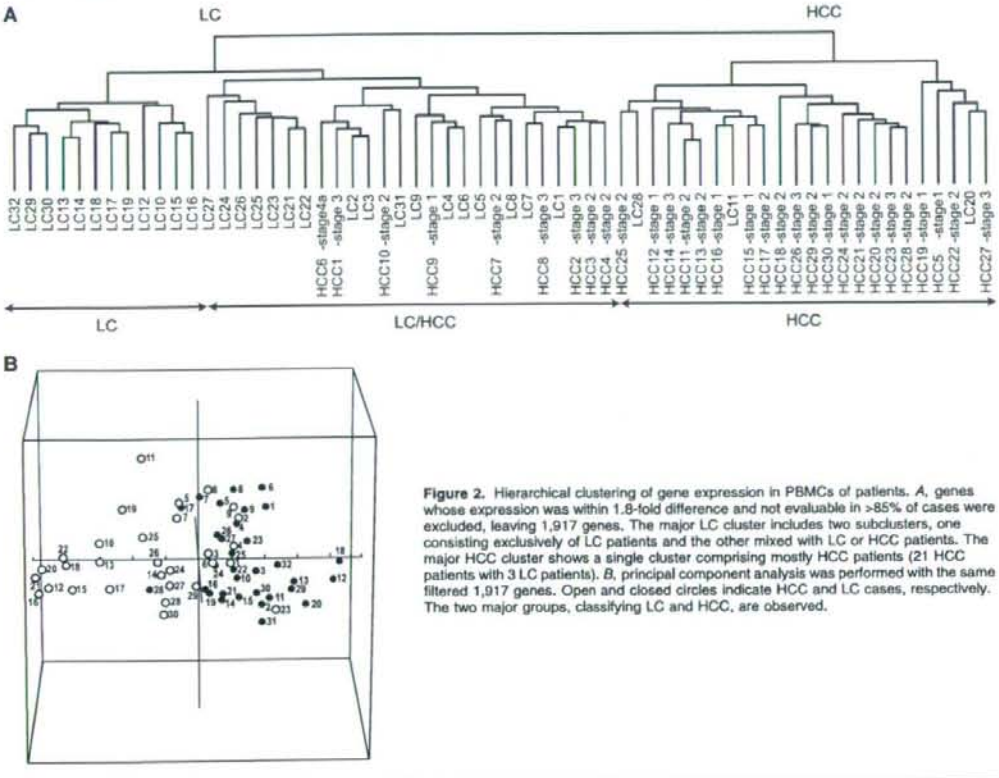

Figure 2. Hierarchical clustering of gene expression in PBMCs of patients. *A*, genes whose expression was within 1.8-fold difference and not evaluable in >85% of cases were excluded, leaving 1,917 genes. The major LC cluster includes two subclusters, one consisting exclusively of LC patients and the other mixed with LC or HCC patients. The major HCC cluster shows a single cluster comprising mostly HCC patients (21 HCC patients with 3 LC patients). *B*, principal component analysis was performed with the same filtered 1,917 genes. Open and closed circles indicate HCC and LC cases, respectively. The two major groups, classifying LC and HCC, are observed.

down-regulated genes were observed, we used MetaCore. The up-regulated genes in PBMCs from patients with HCC were involved in processes such as ubiquitin-proteasomal proteolysis (e.g., heat shock 70 kDa protein 4, ubiquitin conjugating enzymes), mRNA processing (e.g., heterogeneous nuclear ribonucleoproteins, RNA methyltransferase), antigen presentation (e.g., MHC class I polypeptide-related sequence A, B), cell cycle (e.g., HAT1, PCNA), and the response to hypoxia and oxidative stress (e.g., glutaredoxin 2, SOD2, thioredoxin; Table 3). These differentially up-regulated biological processes were also up-regulated processes in HCC-infiltrating inflammatory cells (Table 1). Thus, PBMCs from HCC patients present antigens in conditions of hypoxia and oxidative stress. Additionally, genes involved in other processes, such as apoptosis (e.g., apoptotic peptidase activating factor 1,

Table 2. Supervised learning methods for gene expression of PBMCs

Classifier category	Clinical groups	Total no. cases	No. cases misclassified	Classifier *P* values	No. genes in the classifiers ($P < 0.002$)
LC-C versus HCC	LC-C	32	8	<0.0005	1,430
	HCC	30	2		
Age (y)	>68	31	12	0.317	32
	≤68	31	16		
Gender	Male	25	15	0.178	20
	Female	37	9		
ALT (IU/L)	>50	26	20	0.82	28
	≤50	36	14		
AFP (ng/mL)	>20	29	10	0.02	301
	≤20	33	10		

Table 3. Biological processes for genes up-regulated in PBMCs of HCC patients

Biological process	−log(*P*)	Gene	ID	*t* (T/NT)	*P*	Cellular components
Ubiquitin-proteasomal proteolysis and ER	22.237	Ubiquitin specific peptidase 8	D29956	5.54	0.0000	
		Protein phosphatase 3 (formerly 2B),	NM_000945	4.90	0.0000	
		Heat shock transcription factor 2	NM_004506	4.52	0.0000	
		Heat shock 90 kDa protein 1	NM_005348	4.45	0.0000	T, M
		Ubiquitin protein ligase E3A	NM_000462	4.27	0.0001	
		Ubiquitin-conjugating enzyme E2D1	NM_003338	3.62	0.0006	M
		Phosphatidylinositol glycan, class B	NM_004855	3.57	0.0007	
		Ubiquitin-conjugating enzyme E2D2	NM_003339	3.49	0.0009	
		Ubiquitin-conjugating enzyme E2D3	NM_003340	3.18	0.0023	
		RAN binding protein 2	NM_006267	3.11	0.0029	
		Ubiquitin-conjugating enzyme E2A	NM_003336	3.09	0.0030	
		Activating transcription factor 6	NM_007348	3.03	0.0037	T, M
		Ubiquitin specific protease 7	NM_003470	2.92	0.0050	
		Heat shock 70 kDa protein 9B	NM_001746	2.91	0.0050	
		T-complex 1	NM_030752	2.76	0.0077	
		Glutaredoxin 2	NM_016066	2.70	0.0093	
		Ubiquitin-conjugating enzyme E2N	NM_003348	2.68	0.0096	
		Ubiquitin-conjugating enzyme E2 variant 2	AF049140	2.66	0.0110	
		Ubiquitin specific protease 14	NM_005151	2.20	0.0322	
		Progesterone receptor-associated p48 protein	NM_003932	2.16	0.0353	
		Heat shock 70 kDa protein 4	AB023420	2.16	0.0346	
		Ubiquitin-conjugating enzyme E2L 3	NM_003347	2.14	0.0363	
		Tenascin XB	NM_004381	2.13	0.0377	
		Ubiquitin specific peptidase 33	AB029020	2.12	0.0385	M
mRNA processing	20.087	Heterogeneous nuclear ribonucleoprotein R	NM_005826	3.90	0.0003	T
		RNA (guanine-7-) methyltransferase	NM_003799	3.29	0.0024	
		Heterogeneous nuclear ribonucleoprotein D-like	NM_031372	3.23	0.0020	
		Survival motor neuron domain containing 1	NM_005871	3.12	0.0031	
		Ribonueclease, rnase a family, 4	NM_002937	2.93	0.0052	
		Heterogeneous nuclear ribonucleoprotein A1	NM_002136	2.68	0.0094	
		Heterogeneous nuclear ribonucleoprotein K	NM_002140	2.46	0.0170	
		Heterogeneous nuclear ribonucleoprotein U	NM_031844	2.36	0.0216	
		UPF3, yeast, homologue of, A	NM_023011	2.35	0.0228	
		Alternative splicing factor	M72709	2.03	0.0471	
Antigen presentation	10.124	Janus kinase 1	NM_002227	3.38	0.0013	
		MHC, class II, DO α	NM_002119	3.09	0.0031	
		MHC, class II, DR α	NM_019111	2.67	0.0098	
		MHC class I polypeptide-related sequence B	NM_005931	2.60	0.0122	
		MHC class I polypeptide-related sequence A	NM_000247	2.26	0.0276	
		Tumor necrosis factor receptor–associated factor 6	NM_004620	2.05	0.0456	
Cell Cycle	6.185	Karyopherin (importin) β 2	NM_002270	4.32	0.0001	
		Histone acetyltransferase 1	NM_003642	4.15	0.0001	T, M
		V-myc myelocytomatosis viral oncogene homologue	NM_002467	3.57	0.0008	
		Transforming, acidic coiled-coil containing protein 1	NM_006283	3.38	0.0014	

(*Continued on the following page*)

Table 3. Biological processes for genes up-regulated in PBMCs of HCC patients (Cont'd)

Biological process	−log(*P*)	Gene	ID	*t* (T/NT)	*P*	Cellular components
		Centromere protein B, 80 kDa	X05299	3.37	0.0014	
		Conductin	AF078165	3.07	0.0032	
		Amyloid β precursor protein-binding protein 1	NM_003905	2.99	0.0040	T
		Centromere protein C 1	NM_001812	2.90	0.0054	
		Heterochromatin-like protein 1	BC000954	2.72	0.0085	
		Mature T-cell proliferation 1	BC002600	2.49	0.0154	
		Proliferating cell nuclear antigen	NM_002592	2.46	0.0166	
		CSE1 chromosome segregation 1-like	NM_001316	2.42	0.0186	M
		Karyopherin α4 (importin α3)	NM_002268	2.37	0.0209	
		Signal transducers and activators of transcription–like protein	BC010854	2.36	0.0214	
		M-phase phosphoprotein 6	NM_005792	2.34	0.0228	
		Extra spindle pole bodies homologue 1	NM_012291	2.20	0.0316	
Apoptosis	4.811	Cathepsin S	NM_004079	5.59	0.0000	M
		YME1-like 1	NM_014263	5.49	0.0000	T, M
		Cullin 5	NM_003478	4.65	0.0000	M
		Apoptotic peptidase activating factor 1	NM_001160	3.53	0.0008	
		Cullin 2	NM_003591	3.43	0.0012	M
		Amyloid β precursor protein-binding protein 1	NM_003905	2.99	0.0040	T
		Caspase 9	NM_032996	2.96	0.0044	
		F-box only protein 5	NM_012177	2.88	0.0055	
		Cullin 1	NM_003592	2.52	0.0146	
		Caspase 4	NM_001225	2.23	0.0293	
		Caspase 1	NM_033293	2.02	0.0475	
TCR signaling and immune related	5.462	Protein tyrosine phosphatase, receptor type, C	NM_002838	5.72	0.0000	
		Phosphoinositide-3-kinase, catalytic, α polypeptide	NM_006218	5.38	0.0000	
		Activating transcription factor 2	NM_001880	3.98	0.0002	
		Chemokine (c-c motif) receptor 1	NM_001295	3.90	0.0003	
		NCK adaptor protein 1	NM_006153	3.18	0.0024	
		Chemokine (c-c motif) receptor 2	NM_000647	2.78	0.0075	
		Toll-like receptor2	NM_003264	2.75	0.0078	
		Inositol 1,4,5-triphosphate receptor, type 1	NM_002222	2.24	0.0290	
		T-cell receptor α-chain	X01403	2.05	0.0452	
Response to hypoxia and oxidative stress	2.655	MAP2K1IP1	NM_021970	6.51	0.0000	
		Glutathione s-transferase θ 2	NM_000854	3.43	0.0011	
		Hypoxia-inducible factor 1, α subunit	NM_001530	2.99	0.0040	
		MAP/ERK kinase kinase 5	NM_005923	2.73	0.0086	
		Glutaredoxin 2	NM_016066	2.70	0.0093	
		Peroxiredoxin 3	NM_006793	2.68	0.0157	
		Catalase	NM_001752	2.50	0.0151	
		Plasma glutathione peroxidase 3 precursor	NM_002084	2.19	0.0329	
		Superoxide dismutase 2	NM_000636	2.10	0.0400	
		Thioredoxin	NM_003329	2.05	0.0186	

caspase 9) and T-cell receptor (TCR) signaling (e.g., CCR1, CCR2, TCR α-chain), were also up-regulated in PBMCs from patients with HCC, suggesting vulnerabilities of PBMCs and activated T-cell signaling, respectively, in HCC development.

Biological processes involving the down-regulated genes in PBMCs from patients with HCC included skeletal muscle development, the estrogen receptor 1 (ESR1) nuclear pathway, NOTCH signaling, feeding, and neurohormones signaling, neurogenesis, leptin signaling, and IL-12, IL-15, and IL-18 signaling (Supplementary Table S4), showing no obvious connection compared with the down-regulated genes in HCC-infiltrating mononuclear inflammatory cells (Supplementary Table S3). These results indicate that HCC development in cirrhotic liver can influence PBMCs, providing distinct transcriptional features of up-regulated genes even during the operable stage of HCCs.

Networks of genes commonly up-regulated or down-regulated in both PBMCs and HCC-infiltrating mononuclear inflammatory cells. Analysis of the gene expression profiles of HCC-infiltrating mononuclear inflammatory cells and PBMCs from HCC patients showed that the development of HCC altered the gene expression of local infiltrating mononuclear inflammatory cells and systemically circulating PBMCs; interestingly, the affected biological processes were largely the same. To further explore these presumed local and systemic influences resulting from HCC development, we examined how individual genes were affected by constructing a network.

We found 773 up-regulated and 750 down-regulated significant genes in HCC-infiltrating mononuclear inflammatory cells compared with noncancerous liver-infiltrating mononuclear inflammatory cells at the $P < 0.05$ level. In PBMC gene expression, we observed 2,111 up-regulated and 2,027 down-regulated genes in the PBMCs of HCC patients, compared with LC patients at the $P < 0.05$ level. Among these genes, 378 were significant in both HCC-infiltrating mononuclear inflammatory cells and PBMCs from patients with HCC (Fig. 3*A*). For these 378 genes commonly altered genes, 70% of them were up-regulated or down-regulated in both HCC-infiltrating mononuclear inflammatory cells and PBMCs from HCC patients, whereas expression of the remaining 30% of them was discordant.

We used MetaCore software to perform network construction for 172 up-regulated and 93 down-regulated genes in both HCC-infiltrating mononuclear inflammatory cells and PBMCs from HCC patients. The signal pathway network revealed three central genes, PCNA (32), SMAD3 (33), and nucleophosmin (34), which were all up-regulated in HCC-infiltrating mononuclear inflammatory cells and PBMCs from HCC patients (Fig. 3*B*). PCNA had interactions with proteasome subunit genes, PSMC2, PSMC6, PSMD12, and thioredoxin and DNA polymerase iota genes. SMAD3 was linked with cyclin-dependent kinase 7 and cyclin G_2 with various genes related to the cell cycle. Nucleophosmin was connected to ubiquitin-conjugating enzyme e2e3 and glutaredoxins. Notably, FOXP3, a marker of regulatory T cells, and Janus-activated kinase 3 (JAK3), related to interleukin signaling (35), were up-regulated and down-regulated, respectively, in HCC-infiltrating mononuclear inflammatory cells and PBMCs from HCC patients in the constructed gene network.

The network constructed for individual genes whose expression was commonly altered in HCC-infiltrating mononuclear inflammatory cells and PBMCs from HCC patients also supported a condition of HCC-related stress. The network also indicated that immune reactions in patients with HCC are complex, because down-regulated JAK3, an interleukin signaling molecule, and up-regulated FOXP3 and SMAD3, known molecules of anticancer immunity, are involved in this network. Biological processes in HCC-infiltrating mononuclear inflammatory cells and PBMCs from HCC patients also included the antigen-presentation process.

Discussion

In this study, we explored gene expression in local infiltrating mononuclear inflammatory cells in HCC and noncancerous liver tissues and in PBMCs obtained from patients with hepatitis C–related LC, with or without HCC. Gene expression profiles of HCC-infiltrating mononuclear inflammatory cells were quite distinct from those of noncancerous liver-infiltrating mononuclear inflammatory cells, showing their differing roles in anticancer immunity. We also investigated gene expression in systemically circulating PBMCs from LC-C patients with or without HCC and found that PBMC gene expression profiles from patients with or without HCC were significantly different. Intriguingly, many biological processes involving the up-regulated genes were shared between HCC-infiltrating mononuclear inflammatory cells and PBMCs from HCC patients, suggesting that the local inflammatory effect evoked by HCC development is systemically projected in the host.

Tumor-infiltrating mononuclear inflammatory cells have been investigated to examine their roles in local cancer tissues. We have selectively obtained aggregates of infiltrating mononuclear inflammatory cells in HCC and noncancerous liver tissues by LCM without contamination of carcinoma or parenchymal cells. We have shown that the process of antigen-presentation (36) is a distinguishing feature for up-regulated genes in HCC-infiltrating mononuclear inflammatory cells compared with noncancerous liver-infiltrating mononuclear inflammatory cells. Consistently, immunohistochemical staining of HCC and noncancerous liver tissues revealed that the HCC-infiltrating mononuclear inflammatory cells are primarily monocytes/macrophages, a lineage of phagocytes and antigen-presenting cells (37). Helper CD4 T cells were also found but seemed to be scattered in the HCC-infiltrating mononuclear inflammatory cells, compared with their intensive accumulation in infiltrating mononuclear inflammatory cells in noncancerous liver tissues. Correspondingly, analysis using a publicly available gene expression database of major leukocytes showed that up-regulated genes in HCC-infiltrating mononuclear inflammatory cells were primarily featured for macrophages and Th1 and Th2 CD4 cells, preconditioned with IL-12 and IL-4, respectively. These findings could be interpreted in that HCC expresses tumor-antigens (38) different from the surrounding noncancerous liver tissues; consequently, phagocytes gather in HCC tissues, take up antigens expressed by HCC tissues, and interact with CD4 cells (39). The scattered distribution and transcriptional features of both the Th1 and Th2 predisposed status of CD4 helper T cells in HCC-infiltrating mononuclear inflammatory cells suggests their versatile inflammatory status in cancer immunity, although there was no obvious shift of the Th1/Th2 balance, which is considered to be important in cancer immunity (40).

Other characteristic biological processes involving the up-regulated genes in HCC-infiltrating mononuclear inflammatory cells included the response to hypoxia and oxidative stress (41), the ubiquitin-proteasome system, cell cycle, mRNA processing, ER, and cytoplasm. The ubiquitin-proteasome system is unique to eukaryotic cells and important in maintaining the normal biological activity of cells, with pleiotropic effects in higher animals (42). The cell cycle requires precise regulation of cyclin-dependent kinase under strict control by ubiquitination and subsequent protein degradation (32). Taken together, these processes involving the up-regulated genes may reflect a protective local response of the host, corresponding to the stress environment of HCC. In this sense, the double-strand break repair gene up-regulation may be interpreted as the cells responding to maintain normal cellular activities although they are exposed to a harmful environment by the HCC (43).

The biological processes involving the up-regulated genes in PBMCs from HCC patients, compared with those from LC-C patients without HCC, were, to a substantial degree, the same, involving the up-regulated genes in HCC-infiltrating mononuclear

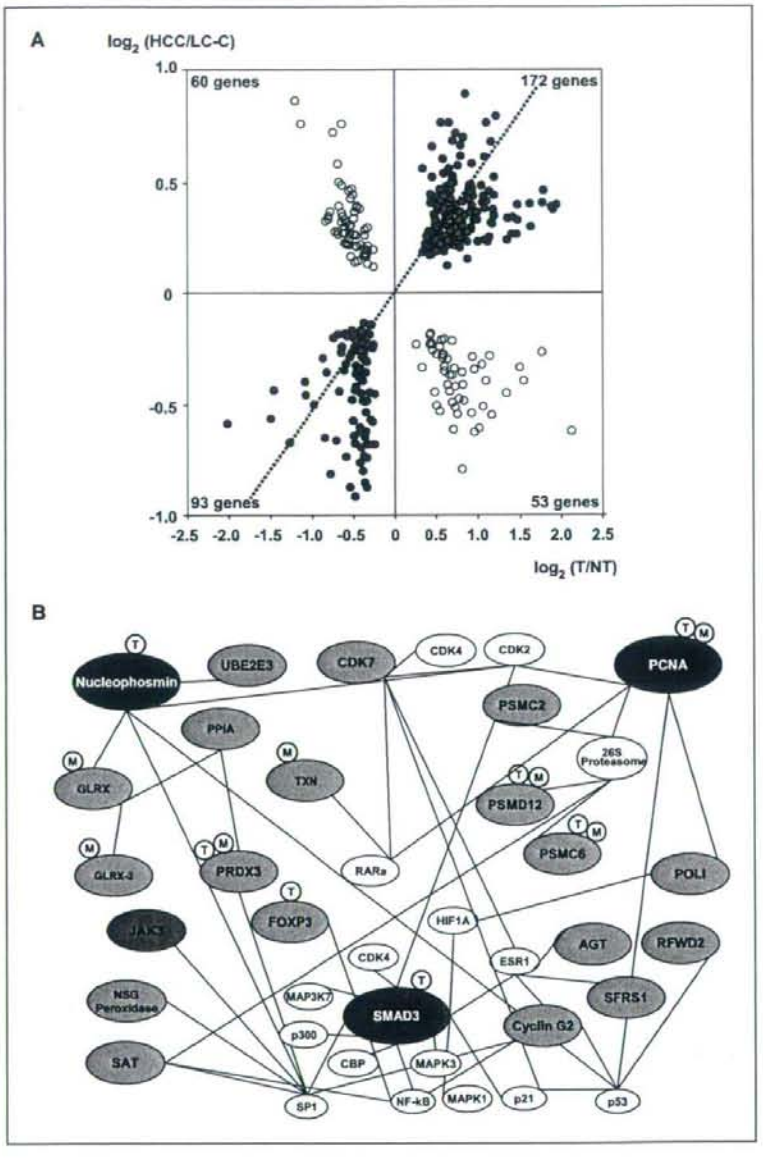

Figure 3. Features of commonly affected genes in PBMCs of HCC patients and HCC-infiltrating mononuclear inflammatory cells. *A*, scatter plots of gene expression ratios between local infiltrating mononuclear inflammatory cells and PBMCs. The axes show the binary logarithm value of the gene expression ratio of HCC-infiltrating mononuclear inflammatory cells over noncancerous liver-infiltrating mononuclear inflammatory cells on the *x* axis and the ratio of PBMCs from HCC patients over LC-C patients on the *y* axis. The right top quadrant includes 172 genes whose expression was up-regulated in HCC-infiltrating mononuclear inflammatory cells and in PBMCs from HCC patients, whereas the left bottom quadrant includes 93 genes down-regulated in both. *B*, interactive network for differentially expressed genes between PBMCs of HCC and LC-C patients and between infiltrating cells adjacent to HCC and noncancerous liver tissues. The three highlighted genes are PCNA, SMAD3, and nucleophosmin, which are related to the redox system, ubiquitin-proteasome system, and cell cycle, in addition to some immunologic gene connections. T or M at each node represent T lymphocytes or monocytes, respectively, and indicate the cell population in which each gene was expressed. The red-filled and blue-filled circles indicate up-regulation or down-regulation, respectively, in HCC-infiltrating mononuclear inflammatory cells and PBMCs from HCC patients.

inflammatory cells, such as ubiquitin-proteasomal proteolysis, ER, and cytoplasm, mRNA processing, antigen presentation, the cell cycle, and the response to hypoxia and oxidative stress. The reflection of these transcriptional features of HCC-infiltrating mononuclear inflammatory cells by PBMCs from HCC patients suggests a systemically projected influence of local HCC development, which is presumably the result of the stress environment caused by HCC and the host's reaction even when the size of the tumor is relatively small. In addition to exploring these biological processes, we also constructed networks of individual genes, the expression of which was similarly up-regulated or down-regulated, to depict commonly affected biological processes in tumor-infiltrating mononuclear inflammatory cells and PBMCs under HCC development in more detail. The networks highlighted three central genes, nucelophosmin, PCNA, and SMAD3, as up-regulated genes. They are connected to individual genes involved in ubiquitin,

proteasomes, the cell cycle, and oxidative stress (Fig. 3*B*). Interestingly, the immunologically important molecules, FOXP3 and JAK3, are in the network as up-regulated and down-regulated genes, respectively. FOXP3 is a transcriptional marker for regulatory T cells (44), and SMAD3 is also believed to be important in maintaining regulatory T cells (45). JAK3, which is associated with the interleukin receptor common γ chain (35) and is important in lymphoid development (46), was also involved in the network, suggesting that HCC influences the host immune system, which can be observed not only in HCC-infiltrating mononuclear inflammatory cells but also in the PBMCs of HCC patients. Thus, the network features of individual genes, commonly affected in HCC-infiltrating mononuclear inflammatory cells and PBMCs from HCC patients, further imply that the anticancer immunity of the host in response to HCC development involves the antigen presentation process to initiate the immune reaction.

The mechanism by which PBMCs from HCC patients reflect the transcriptional features of HCC-infiltrating mononuclear inflammatory cells requires further study. We observed that the population of CCR1-expressing and CCR2-expressing cells in PBMCs from HCC patients was higher than in those from LC-C patients. However, HCC-infiltrating mononuclear inflammatory cells did not show up-regulation of these genes. The meaning of the up-regulated CCR1 and CCR2 should be further investigated because chemokines are key molecules for the recruitment of inflammatory cells, regulating cellular adhesion and transendothelial migration, and the activation of inflammatory cells (47). The biological process of integrin-mediated cell matrix adhesion, genes involved in which were down-regulated in HCC-infiltrating mononuclear inflammatory cells, may suggest that these cells were able to remigrate into the microcirculation with the enriched blood flow in HCC tissues. The process of integrin-mediated cell matrix adhesion in HCC-infiltrating inflammatory cells may imply weaker adhesion of infiltrating mononuclear inflammatory cells to cancer tissues compared with noncancerous liver tissues (48). PBMCs are also presumed to be affected by humoral factors from HCC tissues (49). Another possibility is the presence of hematogenous spreading and circulating HCC cells because mRNA for AFP was detected in circulation (50). Because two-thirds of HCC patients enrolled for gene expression analysis of PBMCs showed serum AFP value <100, the presence of circulating HCC cells would not be evaluated by the detection of *Afp* gene expression alone. Therefore, we have examined expression of *Krt8*, *Krt18*, and *Krt19*, as well as *Afp*. Despite of the possibility of circulating cancer cells, we neither detected expression of *Afp* nor found significantly different expression of *Krt8*, *Krt18*, and *Krt19* between HCC and LC-C patients without HCC. Furthermore, genes up-regulated in HCC tissues compared with noncancerous liver tissues[3] did not correlate to up-regulated genes in PBMCs of HCC patients, indicating that different signature of gene expression in PBMCs between HCC and LC-C patients is not the reflection of the possible migrating cells from HCC tissues. In addition, all HCC cases, except for a case in gene expression analysis of PBMCs, were radiologically free of tumor thrombus in the vessel, which was indicative of microscopic invasion free or concomitant with invasion in the periphery of third or lower branch of vessels, suggesting that contribution of circulating cancer cells were presumed to be sufficiently small for the distinct difference of gene expression signature of PBMCs.

Although the number of enrolled HCC patients for analysis with local inflammatory cells was relatively small compared with the number of patients for analysis of PBMCs, our study has shown shared features of gene expression profiles of HCC-infiltrating mononuclear inflammatory cells and PBMCs from HCC patients, showing a complex immune status of the host in anticancer immunity. This finding suggests the possibility that readily accessible PBMCs can be used as a surrogate tissue to assess the local inflammatory environment surrounding cancers through examination of gene expression profiles.

Disclosure of Potential Conflicts of Interest

No potential conflicts of interest were disclosed.

Acknowledgments

Received 3/10/2008; revised 9/5/2008; accepted 9/25/2008.

The costs of publication of this article were defrayed in part by the payment of page charges. This article must therefore be hereby marked *advertisement* in accordance with 18 U.S.C. Section 1734 solely to indicate this fact.

We thank Nakamura for her invaluable contribution to this study.

[3] Unpublished data.

References

1. El-Serag HB, Mason AC. Rising incidence of hepatocellular carcinoma in the United States. N Engl J Med 1999;340:745–50.
2. Motola-Kuba D, Zamora-Valdes D, Uribe M, Mendez-Sanchez N. Hepatocellular carcinoma. An overview. Ann Hepatol 2006;5:16–24.
3. Yoshida H, Shiratori Y, Moriyama M, et al. Interferon therapy reduces the risk for hepatocellular carcinoma: national surveillance program of cirrhotic and noncirrhotic patients with chronic hepatitis C in Japan. IHIT Study Group. Inhibition of Hepatocarcinogenesis by Interferon Therapy. Ann Intern Med 1999;131:174–81.
4. Farinati F, Marino D, De Giorgio M, et al. Diagnostic and prognostic role of α-fetoprotein in hepatocellular carcinoma: both or neither? Am J Gastroenterol 2006; 101:524–32.
5. Yu P, Lee Y, Liu W, et al. Priming of naive T cells inside tumors leads to eradication of established tumors. Nat Immunol 2004;5:141–9.
6. Preynat-Seauve O, Schuler P, Contassot E, Beermann F, Huard B, French LE. Tumor-infiltrating dendritic cells are potent antigen-presenting cells able to activate T cells and mediate tumor rejection. J Immunol 2006;176: 61–7.
7. Kawata A, Une Y, Hosokawa M, Uchino J, Kobayashi H. Tumor-infiltrating lymphocytes and prognosis of hepatocellular carcinoma. Jpn J Clin Oncol 1992;22:256–63.
8. Hirano S, Iwashita Y, Sasaki A, Kai S, Ohta M, Kitano S. Increased mRNA expression of chemokines in hepatocellular carcinoma with tumor-infiltrating lymphocytes. J Gastroenterol Hepatol 2007;22:690–6.
9. Kobayashi N, Hiraoka N, Yamagami W, et al. FOXP3+ regulatory T cells affect the development and progression of hepatocarcinogenesis. Clin Cancer Res 2007;13: 902–11.
10. Williams MA, Newland AC, Kelsey SM. The potential for monocyte-mediated immunotherapy during infection and malignancy: Part I. Apoptosis induction and cytotoxic mechanisms. Leuk Lymphoma 1999;34:1–23.
11. Nakao M, Sata M, Saitsu H, et al. CD4+ hepatic cancer-specific cytotoxic T lymphocytes in patients with hepatocellular carcinoma. Cell Immunol 1997;177: 176–81.
12. Honda M, Kawai H, Shirota Y, Yamashita T, Kaneko S. Differential gene expression profiles in stage I primary biliary cirrhosis. Am J Gastroenterol 2005;100:2019–30.
13. Honda M, Yamashita T, Ueda T, Takatori H, Nishino R, Kaneko S. Different signaling pathways in the livers of patients with chronic hepatitis B or chronic hepatitis C. Hepatology 2006;44:1122–38.
14. Daiba A, Inaba N, Ando S, et al. A low-density cDNA microarray with a unique reference RNA: pattern recognition analysis for IFN efficacy prediction to HCV as a model. Biochem Biophys Res Commun 2004;315:1088–96.
15. Tateno M, Honda M, Kawamura T, Honda H, Kaneko S. Expression profiling of peripheral-blood mononuclear cells from patients with chronic hepatitis C undergoing interferon therapy. J Infect Dis 2007;195:255–67.
16. Takamura T, Honda M, Sakai Y, et al. Gene expression profiles in peripheral blood mononuclear cells reflect the pathophysiology of type 2 diabetes. Biochem Biophys Res Commun 2007;361:379–84.
17. Burczynski ME, Twine NC, Dukart G, et al. Transcriptional profiles in peripheral blood mononuclear cells prognostic of clinical outcomes in patients with advanced renal cell carcinoma. Clin Cancer Res 2005;11: 1181–9.

18. Matsui O. Imaging of multistep human hepatocarcinogenesis by CT during intra-arterial contrast injection. Intervirology 2004;47:271–6.
19. Sakai Y, Morrison BJ, Burke JD, et al. Vaccination by genetically modified dendritic cells expressing a truncated neu oncogene prevents development of breast cancer in transgenic mice. Cancer Res 2004;64:8022–8.
20. Wada Y, Nakashima O, Kutami R, Yamamoto O, Kojiro M. Clinicopathological study on hepatocellular carcinoma with lymphocytic infiltration. Hepatology 1998;27:407–14.
21. Fu J, Xu D, Liu Z, et al. Increased regulatory T cells correlate with CD8 T-cell impairment and poor survival in hepatocellular carcinoma patients. Gastroenterology 2007;132:2328–39.
22. Xu W, Roos A, Daha MR, van Kooten C. Dendritic cell and macrophage subsets in the handling of dying cells. Immunobiology 2006;211:567–75.
23. Gadola SD, Dulphy N, Salio M, Cerundolo V. Vα24-JαQ-independent, CD1d-restricted recognition of α-galactosylceramide by human CD4(+) and CD8αβ(+) T lymphocytes. J Immunol 2002;168:5514–20.
24. Feinberg H, Taylor ME, Weis WI. Scavenger receptor C-type lectin binds to the leukocyte cell surface glycan Lewis(x) by a novel mechanism. J Biol Chem 2007;282:17250–8.
25. Orabona C, Grohmann U, Belladonna ML, et al. CD28 induces immunostimulatory signals in dendritic cells via CD80 and CD86. Nat Immunol 2004;5:1134–42.
26. Demartino GN, Gillette TG. Proteasomes: machines for all reasons. Cell 2007;129:659–62.
27. Petruti-Mot AS, Earnshaw WC. Two differentially spliced forms of topoisomerase IIα and β mRNAs are conserved between birds and humans. Gene 2000;258:183–92.
28. Naryzhny SN, Desouza LV, Siu KW, Lee H. Characterization of the human proliferating cell nuclear antigen physico-chemical properties: aspects of double trimer stability. Biochem Cell Biol 2006;84:669–76.
29. Velazquez RF, Rodriguez M, Navascues CA, et al. Prospective analysis of risk factors for hepatocellular carcinoma in patients with liver cirrhosis. Hepatology 2003;37:520–7.
30. Ikeda K, Arase Y, Saitoh S, et al. Prediction model of hepatocarcinogenesis for patients with hepatitis C virus-related cirrhosis. Validation with internal and external cohorts. J Hepatol 2006;44:1089–97.
31. Tarao K, Rino Y, Ohkawa S, et al. Close association between high serum alanine aminotransferase levels and multicentric hepatocarcinogenesis in patients with hepatitis C virus-associated cirrhosis. Cancer 2002;94:1787–95.
32. Cayrol C, Ducommun B. Interaction with cyclin-dependent kinases and PCNA modulates proteasome-dependent degradation of p21. Oncogene 1998;17:2437–44.
33. Riggins GJ, Thiagalingam S, Rozenblum E, et al. Mad-related genes in the human. Nat Genet 1996;13:347–9.
34. Dhar SK, Lynn BC, Daosukho C, St Clair DK. Identification of nucleophosmin as an NF-κB co-activator for the induction of the human SOD2 gene. J Biol Chem 2004;279:28209–19.
35. Oakes SA, Candotti F, Johnston JA, et al. Signaling via IL-2 and IL-4 in JAK3-deficient severe combined immunodeficiency lymphocytes: JAK3-dependent and independent pathways. Immunity 1996;5:605–15.
36. Smyth MJ, Godfrey DI, Trapani JA. A fresh look at tumor immunosurveillance and immunotherapy. Nat Immunol 2001;2:293–9.
37. Dobrovolskaia MA, Vogel SN. Toll receptors, CD14, and macrophage activation and deactivation by LPS. Microbes Infect 2002;4:903–14.
38. Kim JW, Ye Q, Forgues M, et al. Cancer-associated molecular signature in the tissue samples of patients with cirrhosis. Hepatology 2004;39:518–27.
39. Itano AA, Jenkins MK. Antigen presentation to naive CD4 T cells in the lymph node. Nat Immunol 2003;4:733–9.
40. Budhu A, Wang XW. The role of cytokines in hepatocellular carcinoma. J Leukoc Biol 2006;80:1197–213.
41. Gerald D, Berra E, Frapart YM, et al. JunD reduces tumor angiogenesis by protecting cells from oxidative stress. Cell 2004;118:781–94.
42. Pickart CM. Back to the future with ubiquitin. Cell 2004;116:181–90.
43. Liu L, Simon MC. Regulation of transcription and translation by hypoxia. Cancer Biol Ther 2004;3:492–7.
44. Ramsdell F. Foxp3 and natural regulatory T cells: key to a cell lineage? Immunity 2003;19:165–8.
45. Fantini MC, Becker C, Monteleone G, Pallone F, Galle PR, Neurath MF. Cutting edge: TGF-β induces a regulatory phenotype in CD4+CD25- T cells through Foxp3 induction and down-regulation of Smad7. J Immunol 2004;172:5149–53.
46. Park SY, Saijo K, Takahashi T, et al. Developmental defects of lymphoid cells in Jak3 kinase-deficient mice. Immunity 1995;3:771–82.
47. Baggiolini M. Chemokines and leukocyte traffic. Nature 1998;392:565–8.
48. Leon MP, Bassendine MF, Gibbs P, Thick M, Kirby JA. Immunogenicity of biliary epithelium: study of the adhesive interaction with lymphocytes. Gastroenterology 1997;112:968–77.
49. Cao M, Cabrera R, Xu Y, et al. Hepatocellular carcinoma cell supernatants increase expansion and function of CD4(+)CD25(+) regulatory T cells. Lab Invest 2007;87:582–90.
50. Wong IH, Yeo W, Leung T, Lau WY, Johnson PJ. Circulating tumor cell mRNAs in peripheral blood from hepatocellular carcinoma patients under radiotherapy, surgical resection or chemotherapy: a quantitative evaluation. Cancer Lett 2001;167:183–91.

ELSEVIER

Journal of Hepatology 50 (2009) 100–110

Journal of Hepatology

www.elsevier.com/locate/jhep

Activation of lipogenic pathway correlates with cell proliferation and poor prognosis in hepatocellular carcinoma☆

Taro Yamashita[1], Masao Honda[1,2], Hajime Takatori[1], Ryuhei Nishino[1], Hiroshi Minato[3], Hiroyuki Takamura[4], Tetsuo Ohta[4], Shuichi Kaneko[1,*]

[1] *Department of Gastroenterology, Kanazawa University Graduate School of Medical Science, 13-1 Takara-Machi, Kanazawa 920-8641, Japan*
[2] *Department of Advanced Medical Technology, Kanazawa University School of Health Sciences, 13-1 Takara-Machi, Kanazawa 920-8641, Japan*
[3] *Pathology Section, Kanazawa University Hospital, 13-1 Takara-Machi, Kanazawa 920-8641, Japan*
[4] *Department of Gastroenterologic Surgery, Kanazawa University Graduate School of Medical Science, 13-1 Takara-Machi, Kanazawa 920-8641, Japan*

***Background/Aims*: Metabolic dysregulation is one of the risk factors for the development of hepatocellular carcinoma (HCC). We investigated the activated metabolic pathway in HCC to identify its role in HCC growth and mortality.**

***Methods*: Gene expression profiles of HCC tissues and non-cancerous liver tissues were obtained by serial analysis of gene expression. Pathway analysis was performed to characterize the metabolic pathway activated in HCC. Suppression of the activated pathway by RNA interference was used to evaluate its role in HCC *in vitro*. Relation of the pathway activation and prognosis was statistically examined.**

***Results*: A total of 289 transcripts were up- or down-regulated in HCC compared with non-cancerous liver ($P < 0.005$). Pathway analysis revealed that the lipogenic pathway regulated by sterol regulatory element binding factor 1 (*SREBF1*) was activated in HCC, which was validated by real-time RT-PCR. Suppression of *SREBF1* induced growth arrest and apoptosis whereas overexpression of *SREBF1* enhanced cell proliferation in human HCC cell lines. *SREBF1* protein expression was evaluated in 54 HCC samples by immunohistochemistry, and Kaplan–Meier survival analysis indicated that *SREBF1*-high HCC correlated with high mortality.**

***Conclusions*: The lipogenic pathway is activated in a subset of HCC and contributes to cell proliferation and prognosis.**

***Keywords*: Hepatocellular carcinoma; Serial analysis of gene expression; Lipogenesis; Gene expression profiling; Sterol regulatory element binding factor 1**

Received 26 May 2008; received in revised form 1 July 2008; accepted 23 July 2008; available online 12 October 2008
Associate Editor: J.M. Llovet

☆ The authors who have taken part in the research of this paper declared that they do not have a relationship with the manufacturers of the materials involved either in the past or present and they did not receive funding from the manufacturers to carry out their research.

* Corresponding author. Tel.: +81 76 265 2231; fax: +81 76 234 4250.
E-mail address: skaneko@m-kanazawa.jp (S. Kaneko).

Abbreviations: HCC, hepatocellular carcinoma; *SREBF1*, sterol regulatory element binding factor 1; HBV, hepatitis B virus; HCV, hepatitis C virus; SAGE, serial analysis of gene expression; RT-PCR, reverse transcription-polymerase chain reaction; IHC, immunohistochemistry; FADS1, fatty acid desaturase 1; SCD, stearoyl CoA desaturase; FASN, fatty acid synthase; si-RNA, short interfering-RNA; CLD, chronic liver disease; PCNA, proliferating cell nuclear antigen; IGF, insulin-like growth factor.

1. Introduction

Hepatocellular carcinoma (HCC) is one of the most frequently occurring malignancies in the world [1]. The major risk factors associated with HCC include chronic infection with hepatitis B virus (HBV) and hepatitis C virus (HCV), alcohol abuse, and exposure to aflatoxin B1 [2]. HCC usually develops from liver cirrhosis, which involves continuous inflammation and hepatocyte regeneration, suggesting that reactive oxygen species and DNA damage are involved in the process of hepatocarcinogenesis [3].

The development of gene expression profiling technologies including DNA microarrays and serial analysis

0168-8278/$34.00
doi:10.1016/j.jhep.2008.07.036

of gene expression (SAGE) have enhanced our ability to identify inventory transcripts and global genetic alterations in HCC [4–10]. In general, these methods have demonstrated that transcripts associated with cell growth are up-regulated, whereas those related to inhibition of cell growth are down-regulated, in HCC [11]. It is difficult, however, to decipher molecular pathways activated during hepatocarcinogenesis.

Epidemiological studies suggest that metabolic dysregulation in the liver increases the risk of HCC development. For example, diabetes is associated with a 2-fold increase in the risk of HCC [12]. Obesity and hepatic steatosis also increase the risk of HCC [13–15]. Furthermore, recent studies indicate that HCV infection provokes hepatic steatosis, which may be a vulnerable factor for liver inflammation and HCC development [16,17]. Thus, dysregulation of a metabolic pathway may play a crucial role to promote HCC growth, but the molecular mechanism is still obscure. In this study, we have utilized SAGE [18,19], which enables us to monitor the differential expression of all genes, to determine the global changes in gene expression that occur during hepatocarcinogenesis.

2. Materials and methods

2.1. Tissue samples

All HCC tissues, adjacent non-cancerous liver tissues, and normal liver tissues were obtained from 69 patients who underwent hepatectomy from 1997 to 2005 in Kanazawa University Hospital. Normal liver tissue samples were obtained from patients undergoing surgical resection of the liver for treatment of metastatic colon cancer. HCC and surrounding non-cancerous liver samples were obtained from patients undergoing surgical resection of the liver for the treatment of HCC. The samples used for SAGE, real-time reverse-transcription (RT)-PCR analysis, and immunohistochemistry (IHC) are listed in Supplemental Table 1. All samples used for SAGE and real-time RT-PCR analysis were snap-frozen in liquid nitrogen. Four normal liver tissues and 20 HCCs and their corresponding non-cancerous liver tissues were used for real-time RT-PCR analysis; seven of these HCC samples, along with 47 additional HCC samples, were formalin-fixed paraffin-embedded and used for IHC. HCC and adjacent non-cancerous liver were histologically characterized as described [20].

All strategies used for gene expression analysis as well as tissue acquisition processes were approved by the Ethics Committee and the Institutional Review Board of Kanazawa University Hospital. All procedures and risks were explained verbally, and each patient provided written informed consent.

2.2. SAGE

Total RNA was purified from each homogenized tissue sample using a ToTally RNA extraction kit (Ambion, Inc., Austin, TX), and polyadenylated RNA was isolated using a MicroPoly (A) Pure kit (Ambion). A total of 2.5 μg mRNA per sample was analyzed by SAGE [18]. SAGE libraries were randomly sequenced at the Genomic Research Center (Shimadzu-Biotechnology, Kyoto, Japan), and the sequence files were analyzed with SAGE 2000 software. The size of each SAGE library was normalized to 300,000 transcripts per library, and the abundance of transcripts was compared by SAGE 2000 software. Monte Carlo simulation was used to select genes with significant differences in expression between two libraries without multiple hypothesis testing correction ($P < 0.005$) [21]. Each SAGE tag was annotated using a gene-mapping web site (http://www.ncbi.nlm.nih.gov/SAGE/index.cgi).

2.3. Analysis of signaling networks

Ingenuity Pathways Analysis software (Ingenuity® Systems, www.ingenuity.com) was used to investigate the molecular pathways activated in an HCC SAGE library compared with an adjacent non-cancerous liver SAGE library. All reliable transcripts statistically up-regulated in HCC were investigated and annotated with biological processes, protein-protein interactions, and gene regulatory networks, using a reference-based data file with statistical significance. All identified pathways were screened individually. MetaCore™ software (GeneGo Inc., St. Joseph, MI) was used to evaluate candidate transcription factors responsible for up-regulation of transcripts in HCC.

2.4. RT-PCR

A 1-μg aliquot of each total RNA was reverse-transcribed using SuperScript II reverse-transcriptase (Invitrogen, Carlsbad, CA). Real-time RT-PCR analysis was performed using ABI PRISM 7900 Sequence Detection System (Applied Biosystems, Foster City, CA). Using the standard curve method, quantitative PCR was performed in triplicate for each sample-primer set. Each sample was normalized relative to β-actin. The assay IDs used were Hs00231674_m1 for sterol regulatory element binding factor 1 (*SREBF1*); Hs00203685_m1 for fatty acid desaturase 1 (*FADS1*) ;Hs00748952_s1 for stearoyl CoA desaturase (*SCD*); Hs00188012_m1 for fatty acid synthase (*FASN*); and Hs99999_m1 for β-actin. *SREBF1a* and *SREBF1c* mRNA levels were assayed by semi-quantitative RT-PCR [22].

2.5. RNA Interference targeting SREBF1

Si-RNAs targeting *SREBF1* were constructed using a *Silencer*™ SiRNA Construction kit (Ambion) according to the manufacturer's protocol. We constructed two different si-RNAs, targeting different sites of *SREBF1* (*SREBF1*-1; CAGTGGCACTGACTCTTCC, *SREBF1*-2; TCTACGACCAGTGGGACTG). Control si-RNA duplexes targeting scramble sequences were also synthesized (Dharmacon Research, Inc., Lafayette, CO). Lipofectamine 2000™ reagent (Invitrogen) was used for transfection according to the manufacturer's instructions.

2.6. Cell proliferation assay

Cell proliferation assays were performed using a Cell Titer96 Aqueous kit (Promega, Madison, WI). Results are expressed as the mean optical density (OD) of each five-well set. All experiments were repeated at least twice.

2.7. Soft agar assay

To each well of a six-well plate, containing a base layer of 0.72% agar in growth medium, was added 1×10^4 cells, suspended in 2 ml of 0.36% agar with growth medium (DMEM supplemented with 10% FBS), and the plates were incubated at 37 °C in a 5% CO_2 incubator for 2 weeks. The numbers of colonies in each well were counted as previously described [23].

2.8. TUNEL assay

A DeadEnd™ Colorimetric TUNEL System (Promega) was used to measure nuclear DNA fragmentation as described previously [24].

2.9. Annexin V staining

To evaluate apoptotic cell death, Annexin V binding to cell membranes was evaluated using Annexin V-FITC antibodies and FACSCalibur flow cytometer (BD Biosciences, Franklin Lakes, NJ), as described by the manufacturer.

2.10. Focus assay

HuH7 cells and Hep3B cells were transiently transfected with pCMV7 or pCMV7-*SREBF1c* vectors (kindly provided by Dr. Hitoshi Shimano) using Lipofectamine 2000™ reagent (Invitrogen), as described by the manufacturer. A total of 2×10^3 cells were seeded on six-well plates 48 h after transfection, and cultured in usual media with 400 ng/ml of Geneticin for 9 days. The foci were fixed with ice-cold 100% methanol and stained with 0.5% crystal violet solution. All experiments were performed in triplicates.

2.11. Western blotting

Whole cell lysates were prepared using RIPA lysis buffer. Antibodies used were rabbit polyclonal antibodies to phospho-GSK-3β (ser9) (Cell Signaling Technology Inc., Danvers, MA), rabbit anti-sterol regulatory element binding protein-1 (encoded by *SREBF1*) polyclonal antibody H-160 (Santa Cruz Biotechnology, Inc., Santa Cruz, CA), and β-actin (Sigma–Aldrich Japan K.K., Tokyo, Japan). Immune complexes were visualized by enhanced chemiluminescence (Amersham Biosciences Corp., Piscataway, NJ) as described in the manufacturer's protocol.

2.12. Immunohistochemistry

Rabbit anti-*SREBF1* polyclonal antibody H-160 (Santa Cruz Biotechnology, Inc.) and mouse anti-proliferating cell nuclear antigen (PCNA) monoclonal antibody PC10 (Calbiochem, San Diego, CA) were used to evaluate the immunoreactivity of HCC samples, using a DAKO EnVision+™ Kit, as described by the manufacturer. The signal intensity of *SREBF1* was scored as negative, low, or high determined by the representative staining of the normal liver tissue and cirrhotic liver tissue (Supplemental Fig. 1). HCC was referred as *SREBF1*-high if *SREBF1* expression in the tumor was higher than that in the cirrhotic liver tissue. PCNA index was evaluated as previously described [25].

2.13. Statistical analysis

Kruskal–Wallis test was used to compare the differentially expressed genes, as shown by real-time PCR, among normal liver, CLD, and HCC tissues. Mann–Whitney U test was also used to evaluate the statistical significance of differences of gene expression between CLD and HCC tissues. Spearman's correlation coefficient was used to assess correlations between the expression levels of *SREBF1*, *FADS1*, *SCD*, and *FASN*. Univariate Cox proportional hazards regression analysis was used to evaluate the association of gene expression and clinicopathologic parameters with patient outcomes. All statistical analyses were performed using SPSS software (SPSS software package; SPSS Inc., Chicago, IL) and GraphPad Prism software (GraphPad Software Inc., La Jolla, CA).

3. Results

3.1. Gene expression profiling of HCC

We constructed two SAGE libraries from a HCC–HBV tissue and a corresponding non-cancerous tissue (chronic liver disease (CLD)–HBV). We also used two previously described SAGE libraries, from an HCC–HCV sample and a corresponding non-cancerous tissue sample (CLD–HCV) [4]. After excluding tags detected only once in each library, to avoid the contamination of tags derived from sequence errors, we selected 105,288 tags corresponding to the 9731 genes in all libraries. Using Monte Carlo simulation, we compared the differentially expressed transcripts in HCC and corresponding CLD libraries. Compared with their corresponding CLD libraries, there were statistically significant increases or decreases in 140 transcripts in the HCC–HBV library and in 197 transcripts in the HCC–HCV library ($P < 0.005$).

The HCC–HBV library contained one SAGE tag encoding the HBV–X region, which was increased more than 35-fold compared with its expression in the corresponding CLD–HBV library (Supplemental Table 2). We identified two additional SAGE tags, encoding unknown genes (GTTCTAAAGG, GCATTATGAT), which were expressed more than 10-fold in the HCC–HBV library than in the corresponding CLD–HBV library. The HCC–HBV library also contained tags associated with lipogenesis, at greater than 10-fold abundance, in the HCC–HBV library; these including tags for steroyl-CoA desaturase, fatty acid synthase, and fatty acid desaturase 1.

In contrast, SAGE tags associated with the immune response were up-regulated in the HCC–HCV library. These included tags for Th1-type chemokines, including chemokine ligand 10 (C–X–C motif), chemokine ligand 9 (C–X–C motif), and major histocompatibility complex classes IA and IB (Supplemental Table 3). In addition, tags associated with lipogenesis were increased in the HCC–HCV library, including tags for 3-hydroxy-3-methylglutaryl-coenzyme A synthase 1 and cytochrome P450, family 51, subfamily A, polypeptide 1. Taken together, the differential gene expression patterns may exist in HCC–HBV and HCC–HCV. HBV–X and lipogenesis-related genes are activated in HCC–HBV, whereas genes associated with inflammation as well as lipogenesis are activated in HCC–HCV.

3.2. Analysis of molecular pathways activated in HCC

To further characterize the gene expression patterns of HCC–HBV and HCC–HCV, we performed pathway analysis on SAGE data. Using MetaCore™ software, we found that the candidate transcription factors activated were distinct in each HCC library (Table 1). Several of these transcription factors, including NF-κB, c-Myc, c-Jun, and HNF4-α, have been reported to be activated in HCC [26–29]. In addition, our findings indicated that the transcription factor *SREBF1* may be activated in both HCC–HBV and HCC–HCV (to avoid a confusion, we use HUGO symbol *SREBF1* to indicate both gene/protein name).

Table 1
Candidate transcription factors that regulate molecular pathways activated in HCC.

SAGE library	Transcription factor	Molecular processes	*P*-value
HCC–HCV	NF-κB	Antigen presentation Antigen processing Defense response Immune response	0.004
	SREBF1	Cholesterol biosynthesis Lipid biosynthesis β-Glucoside transport Negative regulation of lipoprotein metabolism	0.05
	SP1	Electron transport; drug metabolism Oxygen and reactive oxygen species metabolism Cell-substrate junction assembly; wound healing	0.05
	IRF1	Immune response Antigen presentation; antigen processing Defense response; positive regulation of cell	0.05
HCC–HBV	HNF4-α	Lipid transport Fatty acid metabolism Smooth muscle cell proliferation	0.002
	HNF1	Acute-phase response; lipid transport Negative regulation of lipid catabolism β-Glucoside transport Negative regulation of lipoprotein metabolism	0.01
	SP1	Zinc ion homeostasis; response to biotic stimulus Nitric oxide mediated signal transduction Copper ion homeostasis; fatty acid biosynthesis	0.01
	c-Jun	Progesterone catabolism; progesterone metabolism Regulation of lipid metabolism; Prostaglandin metabolism	0.03
	C/EBP-α	Lipid transport; negative regulation of lipid catabolism Negative regulation of lipoprotein metabolism β-Glucoside transport Positive regulation of interleukin-8 biosynthesis	0.03
	SREBF1	Lipid biosynthesis; fatty acid biosynthesis Fatty acid metabolism Negative regulation of lipid catabolism Negative regulation of lipoprotein metabolism	0.03
	c-Myc	Fatty acid biosynthesis; fatty acid metabolism Fatty acid desaturation; Activation of pro-apoptotic gene products Release of cytochrome c from mitochondria	0.03
	USF1	Fatty acid metabolism Smooth muscle cell proliferation	0.03
	PPAR-α	Fatty acid metabolism Smooth muscle cell proliferation	0.03
	COUP-TFI	Lipid transport Smooth muscle cell proliferation	0.03
	C/EBP-β	Acute-phase response Regulation of interleukin-6 biosynthesis Fat cell differentiation Inflammatory response	0.03

These findings were evaluated by other pathway analysis software, Ingenuity Pathways Analysis (IPA). We applied the signaling network analysis to the transcripts up-regulated in the HCC libraries ($P < 0.005$). We found that the top signaling network activated in HCC–HBV contained several pathways involved in ERK/MAPK signaling, PPAR signaling, linoleic acid metabolism, and fatty acid metabolism (Supplemental Fig. 2A). Similarly, pathways involved in interferon signaling, NF-κB signaling, antigen presentation, PPAR signaling, linoleic acid metabolism, and fatty acid metabolism were included in the top signaling network activated in HCC–HCV (Supplemental Fig. 2B). Consistent with the results of transcription factor analysis by MetaCore™, pathway analysis indicated that *SREBF1* participates in the lipogenesis pathway in both HCC–HBV and HCC–HCV (blue nodes in Supplemental Fig. 2A and B). *SREBF1*, a major regulator of the lipogenesis pathway, binds to sterol regulatory elements on the genome [30], but less is known about its role in

HCC [31]. We therefore focused on the role of *SREBF1* signaling in HCC.

3.3. Validation of SAGE and signaling network analysis

We performed real-time RT-PCR analysis of *SREBF1* and three representative target genes (*SCD*, *FADS1*, and *FASN*) [20] on 44 samples not used for SAGE. We found that the levels of *SREBF1*, *SCD*, and *FASN* mRNAs were higher in HCC tissues and CLD tissues compared with normal liver, and that these differences were statistically significant (Fig. 1A). We further compared the expression of *SREBF1*, *FADS1*, and *FASN* between HCC and non-cancerous liver tissues, and identified the overexpression of *SREBF1* in HCC with statistical significance (Supplemental Fig. 3). Scatter plot analysis showed that the expression levels of *SREBF1* were correlated with those of *FADS1* ($R = 0.57$, $P < 0.0001$), *SCD* ($R = 0.82$, $P < 0.0001$), and *FASN* ($R = 0.74$, $P < 0.0001$) (Fig. 1B).

Since the mammalian genome encodes two *SREBF1* isoforms, *SREBF1a* and *SREBF1c* [22], we performed semi-quantitative RT-PCR with isoform specific primers to determine which of these isoforms was up-regulated in HCC. We found that *SREBF1c* mRNA, but not *SREBF1a* mRNA, was up-regulated in HCC compared with adjacent non-cancerous liver and normal liver tissues (Supplemental Fig. 4A).

3.4. Functional assay of the lipogenesis pathway in cell lines

Although genome-wide expression profiling showed that the lipogenesis pathway was activated in HCC possibly through up-regulation of *SREBF1*, it was not clear that this pathway played a role in HCC growth. To investigate the role of lipogenesis in HCC cell proliferation, we transfected two short interfering (si)-RNAs (*SREBF1*-1 and *SREBF1*-2) targeting *SREBF1* into the HuH7 and Hep3B cells. These cell lines have no chromosome amplification or deletion on 17p11, on which *SREBF1* is located [32]. Transfection of the si-RNA constructs for *SREBF1*-1 or *SREBF1*-2 decreased expression of *SREBF1* 90% and 70%, respectively, and the expression of both *SCD* and *FADS1* 70% and 60%, respectively (Fig. 2A). Because differences in *SREBF1c* and *SREBF1a* *sequence alignments* are very small, we could not design si-RNAs specifically targeting *SREBF1c*. We therefore checked the effect of si-RNAs on the expression of the *SREBF1* isoforms. We found that the expression of *SREBF1c* was relatively more suppressed than that of *SREBF1a* (Supplemental Fig. 4B), which may have been associated with the higher expression of *SREBF1a* than *SREBF1c* in cultured cell lines [25].

We found that the growth of these transfected cells was significantly inhibited at 72 h compared with mock transfected cells (Fig. 2B and Supplemental Fig.5A). Examination of anchorage independent cell growth showed strong suppression by deactivation of the lipogenesis pathway (Fig. 2C). Because insulin-like growth factor (IGF) is known to induce cancer cell proliferation through activation of PI3-kinase signaling followed by *SREBF1* induction, we investigated the effect of *SREBF1* knockdown on IGF2 mediated cell proliferation. Interestingly, *SREBF1* knockdown abrogated the IGF2 dependent cell proliferation (Supplemental Fig. 5B). Moreover, both the TUNEL assay and annexin V staining showed that transfection of *SREBF1* si-RNAs increased apoptosis compared with mock transfected cells (Fig. 2D and E).

We further investigated the role of *SREBF1* overexpression on cell growth *in vitro*. We transiently transfected control pCMV7 plasmids or pCMV7-*SREBF1c* plasmids (Fig. 3A), and cell proliferation was enhanced in *SREBF1* overexpressing cells compared with the control in both HuH7 and Hep3B cells evaluated by focus assay (Fig. 3B and supplemental Fig. 6). Furthermore, overexpression of *SREBF1* intensified the phosphorylation of GSK-3β, one of the major kinase phosphorylated by the activation of IGF signaling, in a dose-dependent manner (Fig. 3C).

3.5. SREBF1 Expression and prognosis

Since the above results indicated that *SREBF1* signaling may play an important role on tumor cell growth, we investigated the relationship between *SREBF1* expression and mortality in 54 HCC patients by IHC. When we examined the expression of *SREBF1* in HCC tissues and adjacent non-cancerous liver tissues, we identified the increase of the cytoplasmic *SREBF1* staining in a subset of HCC (Fig. 4A). We evaluated the expression of *SREBF1* in HCC and classified 4, 30, and 20 HCCs as *SREBF1*-negative, *SREBF1*-low, and *SREBF1*-high HCC, respectively (Fig. 4B and Supplemental Fig. 1). We could not detect any differences of clinico-pathological characteristics between *SREBF1*-high HCC and *SREBF1*-low/-negative HCC including histological steatosis (Supplemental Table4). Since the seven of these HCC samples were also used for real-time RT-PCR analysis, we investigated the relation of *SREBF1* RNA and protein expression (Fig. 4C). *SREBF1*RNA expression was significantly higher in *SREBF1*-high HCC than in *SREBF1*-low/-negative HCC with statistical significance ($P = 0.03$). Then we examined the cell proliferation of these HCC samples by PCNA staining. Notably, PCNA indexes were significantly higher in *SREBF1*-high HCC than *SREBF1*-low/-negative HCC with statistical significance ($P < 0.001$) (Fig. 4D). We further investigated the relationship between *SREBF1*

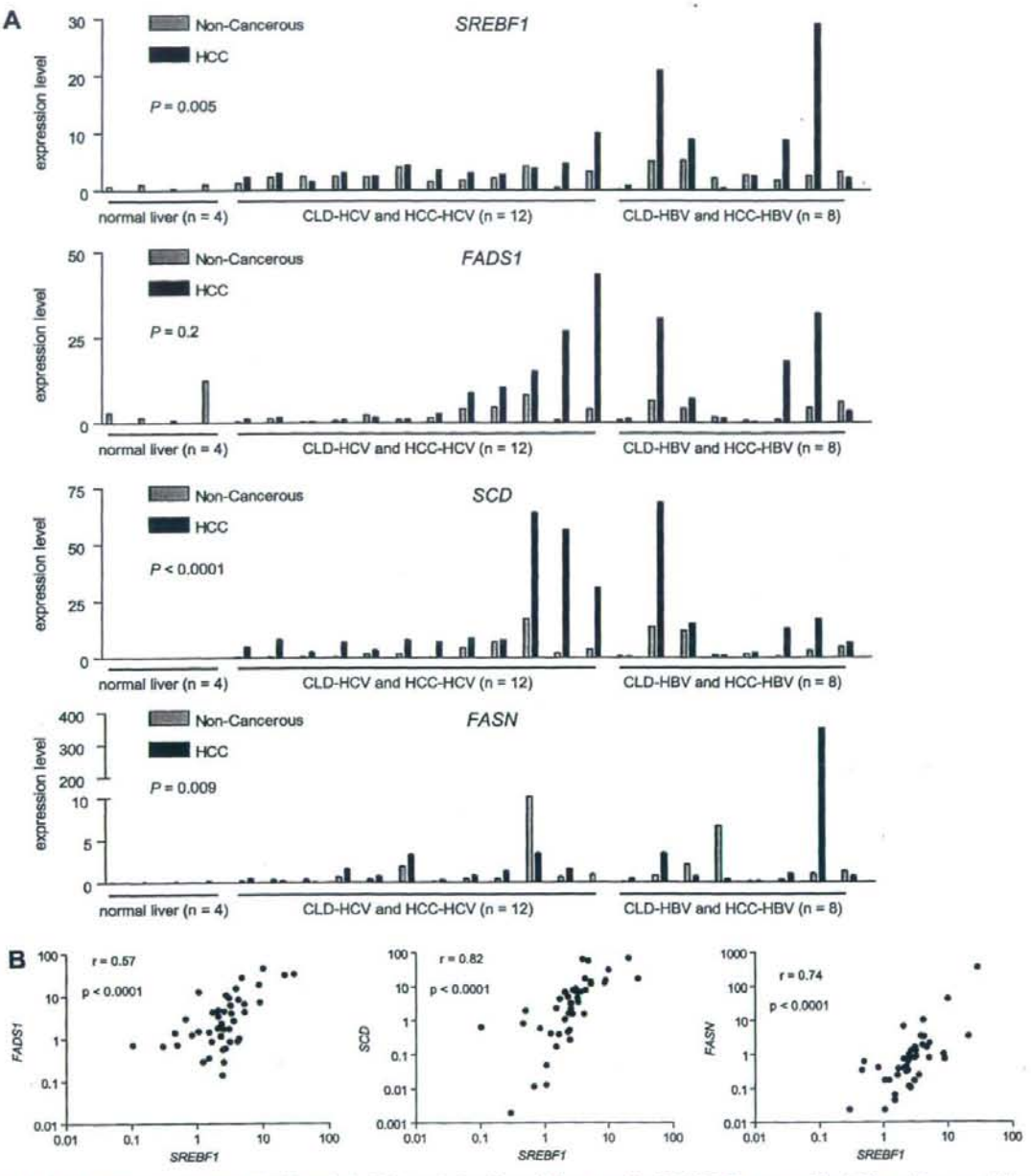

Fig. 1. (A) Real-time quantitative RT-PCR analysis. RNA was isolated from 44 tissue samples: 20 HCC, 20 corresponding CLD, and four normal liver samples. Differential expression of each gene among normal liver tissues, CLD tissues, and HCC tissues was examined by Kruskal–Wallis tests. (B) Scatter plot analysis. Gene expression levels of *FADS1*, *SCD* and *FASN* were well-correlated with those of *SREBF1*, as shown by Spearman's correlation coefficients.

protein expression and prognosis. Kaplan–Meier survival analysis showed a significant relationship between poor survival and high *SREBF1* protein expression ($P = 0.04$; Fig. 4E). Univariate Cox regression analysis showed a correlation between high *SREBF1* protein expression and high risk of mortality with statistical

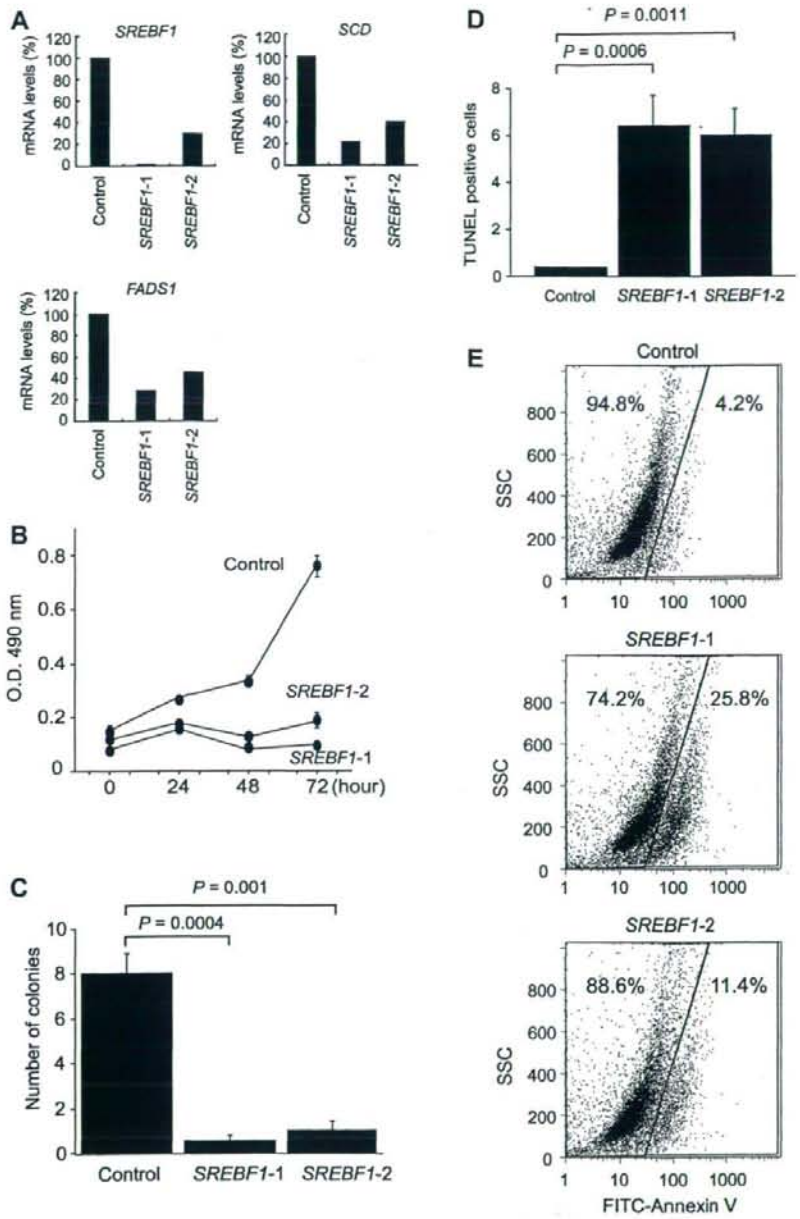

Fig. 2. (A) Effect of RNA interference targeting *SREBF1* in HuH7 cells. Expression levels of *SREBF1* mRNA were reduced by si-RNAs targeting different exons in *SREBF1*. Transcripts of *FADS1* and *SCD* were also down-regulated, showing transcriptional deactivation of the lipogenesis pathway. (B) Cell proliferation assay. Deactivation of the lipogenesis pathway severely reduced cell growth in HuH7 cells. (C) Soft agar assay. Deactivation of the lipogenesis pathway inhibited anchorage independent cell growth in HuH7 cells. (D) TUNEL assay. Deactivation of the lipogenesis pathway significantly increased the number of TUNEL-positive cells in HuH7 cells. (E) Annexin V staining evaluated by flow cytometer. Deactivation of the lipogenesis pathway significantly increased the number of annexin V positive cells in HuH7 cells.

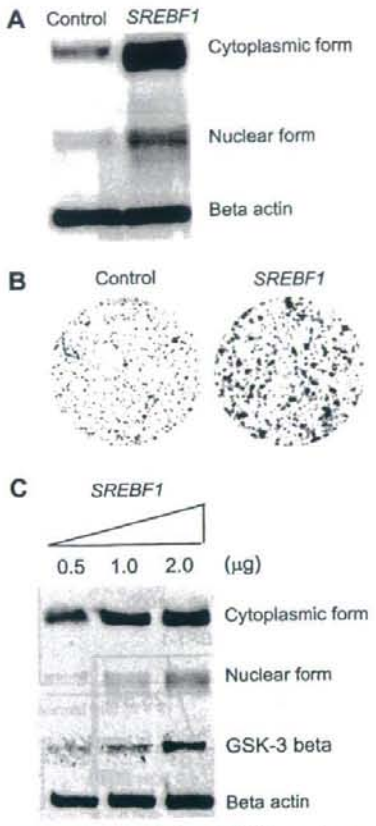

Fig. 3. (A) Western blot analysis of *SREBF1* protein expression in HuH7 cells transfected with control pCMV7 plasmids or pCMV7-*SREBF1c* plasmids. Both cytoplasmic and nuclear forms of *SREBF1* protein expression were increased by pCMV7-*SREBF1c* overexpression. (B) Focus assay of HuH7 cells transfected with control pCMV7 plasmids or pCMV7-*SREBF1c* plasmids. (C) Western blot analysis of *SREBF1* and phospho-GSK-3β protein expression in HuH7 cells transfected with indicated amounts of pCMV7-*SREBF1c* plasmids.

significance (HR, 3.7; 95% CI, 1.0–13.7; $P = 0.05$; Table 2).

4. Discussion

Using large-scale gene expression profiling, we have shown that the lipogenesis pathway is transcriptionally activated in HCC. Our SAGE profiles will be available on our homepage (http://www.intmedkanazawa.jp/) and will be submitted to the Gene Expression Omnibus (http://www.ncbi.nlm.nih.gov/geo/).

We found that the levels of expression of *FADS1*, *SCD*, and *FASN* were each correlated with those of *SREBF1*, suggesting that *SREBF1* is one of the main factors involved in the activation of lipogenesis in HCC. Activation of growth signaling pathways, such as the PI 3-kinase and mitogen-activated protein kinase pathways, has been shown to induce up-regulation of *SREBF1* in prostate and breast cancer cells [33,34]. We have observed induction of *SREBF1* protein expression by IGF2 in HuH7 cells (data not shown). Furthermore, we have identified that *SREBF1* overexpression results in the activation of cell proliferation and PI 3-kinase signaling, whereas expression inhibition of *SREBF1* abrogated the IGF2 induced cell proliferation. Although detailed mechanisms should be clarified in future, our results suggest that *SREBF1* is a key component of PI 3-kinase signaling in HCC.

SREBF1 is induced by alcohol [35], insulin, and fat [30,36], and plays a central role in the mechanism of hepatic steatosis [37]. Interestingly, these *SREBF1* inducers are risk factors for HCC [12,13,38,14]. Strikingly, two recent studies have shown that HBV and HCV infection may also induce hepatic steatosis through activation of *SREBF1* [39,40]. Furthermore, a recent report revealed the activation of *SREBF1* signaling in cancer by hypoxia [41]. Thus, these pathologic conditions such as chronic viral hepatitis, alcohol abuse, obesity, diabetes, and local hypoxia may up-regulate the expression of *SREBF1*, which, in turn, may contribute to an increased risk of hepatocarcinogenesis. Transgenic mice overexpressing *SREBF1* in the liver exhibited hepatic steatosis and hepatomegaly, suggesting the role of *SREBF1* on lipid metabolism and cell proliferation. However, it should be noted that no transgenic mice overexpressing *SREBF1* have been reported to have the risk of HCC development thus far. Interestingly, a recent report indicated that HCV core transgenic mice known to develop HCC showed coordinated activation of lipogenic pathway genes and *SREBF1* [42]. Although further studies are clearly required, we speculate that the activation of *SREBF1* may contribute to promote the development of HCC in already-initiated hepatocytes but not in normal hepatocytes.

Recently, Yahagi et al. reported the activation of lipogenic enzyme related genes in HCC [31]. In that paper, the authors suggested that *SREBF1* expression was not correlated with the expression of other lipogenic genes by Northern blotting, inconsistent with our current data. One possible explanation of these discrepancies might be the different methods for quantitation of mRNA, and we believe that real-time RT-PCR method used in our study would be more accurate. In addition, we evaluated the expression of *SREBF1* and lipogenic genes using more samples (a total of 44 liver and HCC tissues) than Yahagi et al did (10 HCC tissues). Furthermore, a recent paper indicated the coordinated activation of *SREBF1* and lipogenic genes in HCC